


 Cite this: *RSC Adv.*, 2022, 12, 18661

Received 26th April 2022

Accepted 30th May 2022

DOI: 10.1039/d2ra02663e

[rsc.li/rsc-advances](https://rsc.li/rsc-advances)

# Reduction of 4-nitrophenol using green-fabricated metal nanoparticles

 Yetzin Rodriguez Mejía<sup>a</sup> and Naveen Kumar Reddy Bogireddy \*<sup>b</sup>

Noble metal (silver (Ag), gold (Au), platinum (Pt), and palladium (Pd)) nanoparticles have gained increasing attention due to their importance in several research fields such as environmental and medical research. This review focuses on the basic perceptions of the green synthesis of metal nanoparticles and their supported-catalyst-based reduction of 4-nitrophenol (4-NP) to 4-aminophenol (4-AP). The mechanisms for the formation of these nanoparticles and the catalytic reduction of 4-NP are discussed. Furthermore, the parameters that need to be considered in the catalytic efficiency calculations and perspectives for future studies are also discussed.

## 1 Introduction

In recent years, one issue that has generated significant concern due to its adverse effects, mainly on human health, is the contamination of water (surface and groundwater), including the ocean.<sup>1–3</sup> The principal cause of this event is the high amounts of toxic and refractory pollutants, mainly 4-nitrophenol (4-NP),<sup>1,4–6</sup> which is widely used in the pharmaceutical and textile industries<sup>7,8</sup> for the production of herbicides, insecticides, synthetic dyes, and paints, and as a corrosion inhibitor and pH indicator, among other applications.<sup>4,9,10</sup>

Therefore, the reduction of 4-NP to 4-aminophenol (4-AP) has become a crucial issue, given that 4-AP is a compound with a lower degree of toxicity.<sup>6,11</sup> Among the various 4-NP reduction reactions, the reaction with sodium borohydride (NaBH<sub>4</sub>) as a reducing agent (H<sub>2</sub> source) in conjunction with metal catalysts, such as Pd,<sup>12–14</sup> Ag,<sup>15,16</sup> Pt,<sup>8,17</sup> Cu,<sup>18</sup> Au<sup>4,9,19</sup> and their assemblies on dendrimers, polymeric matrices, microgels, metal-immobilized silica-coated supports, and graphene oxide,<sup>20</sup> has gained more attention due to its eco-friendly and straightforward reduction process. Furthermore, chemical and green methods are widely employed for the fabrication of nanomaterials as catalysts for the 4-NP reduction reaction<sup>21</sup> in aqueous and semi-solid media.<sup>5,11,21–23</sup> Pradhan *et al.*<sup>23</sup> primarily introduced 4-NP reduction as a model reaction using Ag nanoparticles. The catalytic reduction reaction was real-time monitored *via* UV-visible spectroscopy by observing the decrease in the absorption band at 400 nm belonging to the 4-

<sup>a</sup>Facultad de Química, Universidad Autónoma del estado de México, Paseo Colón esq. Paseo Tollocan s/n, Toluca, Estado de México, C.P. 50120, Mexico

<sup>b</sup>Instituto de Física, Universidad Nacional Autónoma de México (UNAM), Ciudad de México, C.P. 04510, México. E-mail: naveenbogireddy@fisica.unam.mx; nsbogireddy@gmail.com



Yetzin Rodriguez obtained her Master's Degree in Sustainable Energy from the Autonomous State University of Morelos. She is currently working as a PhD student in Materials Science at the Autonomous State University of Mexico. She was involved in several collaborative projects focused on the production of biofuels and bioremediation at various centers in Mexico. She has experience synthesizing and

characterizing biogenic silica and metal-organic frameworks (MOFs) and their application in water purification and as supports for biocatalysts for the production of biodiesel.



Naveen Kumar Reddy Bogireddy obtained his PhD in Engineering and Applied Sciences with First Class Honors at the Autonomous State University of Morelos. Currently, he is doing a post-doctoral stay at the Institute of Physics-National Autonomous University of Mexico. His work on advanced nanomaterials for environmental applications is going to be consolidated. He has several years of experience in the

fabrication and characterization of metallic nanoparticles and carbon dots and their application for the detection and mitigation of toxic organic pollutants in aqueous media.



nitrophenolate ion (intermediate product) and increase in the band at 300 nm related to 4-AP.<sup>4,22</sup> Subsequently, many studies have been reported, but compared to other techniques, green-synthesized catalysts play a vital role in the 4-NP reduction reaction due to their biocompatibility, low toxicity, low cost, and easy preparation process. Also, several green reducing agents, such as ascorbic acid,<sup>24</sup> formic acid,<sup>23</sup> tetramethyl disiloxane,<sup>25</sup> plant or seed extracts, and microorganisms,<sup>26</sup> have been studied.<sup>19,27–29</sup>

The purpose of this review is to present the scientific advances in the green synthesis of noble metal nanoparticles and their application in the reduction of 4-nitrophenol in aqueous media, clearly explaining the reaction mechanisms of both metal nanoparticle synthesis and 4-NP reduction.

The overall publication trend in the last two decades is presented in Fig. 1. During the first decade (2000 to 2010), only less than 200 articles were published annually. On the contrary, during the second decade (2011 to 2020), a significant increase (almost four-fold higher) in the number of annually published articles was observed. During the pandemic period, many articles were published, which can be explained by the growing recognition and importance of 4-NP.

### 1.1 History of 4-nitrophenol

The three-step procedure to synthesize paracetamol was first proposed by J. von Mering in 1893, which was advertised in 1953 considering that it safer than aspirin. The steps in synthesis of paracetamol are as follows: nitration of phenol → conversion of nitro group (4-NP) → amino group (4-AP) and acetylate amino group → paracetamol (Fig. 2).

4-Nitrophenol is also called *para*-nitrophenol (*p*-nitrophenol) or 4-hydroxynitrobenzene. It has a nitro group at the *para* position in a phenolic compound (*i.e.*, hydroxyl (–OH) group attached to a carbon atom in a benzene ring). In general, it is used in pharmaceutical drugs and insecticides. Moreover, 4-NP

is an intermediate product in the production of acetaminophen (paracetamol) from phenol (as mentioned above). Human beings may be exposed to 4-NP by drinking polluted water.

## 2 Update on 4-nitrophenol reduction using green-synthesized metal nanoparticles

There are few reports on the reduction of 4-nitrophenol. Pengxiang *et al.*,<sup>21</sup> Maryam *et al.*,<sup>22</sup> and Muhammad *et al.*<sup>23</sup> mainly focused on the synthesis-dependent fabrication of AuNPs and their nanocatalyst assemblies to reduce nitrophenol. In this review, we focus on green-fabricated monometallic, bimetallic Ag, Au, Pt, and Pd NPs and their assembled structures to reduce 4-NP using NaBH<sub>4</sub> as the model reaction.

## 3 Catalyst fabrication and characterization

### 3.1 Green synthesis-mediated metal nanoparticles as catalysts

The fabrication of nanoparticles (from different metals) *via* green synthesis has achieved great importance due to the fact that it “reduces” the use and formation of toxic compounds.<sup>29,30</sup> The use of biological materials such as bacteria, fungi, algae, and plant extracts (roots, leaves, fruits, flowers, and seeds)<sup>30–32</sup> avoids the use of intermediate base groups, making it a cost-effective, accessible, eco-friendly, and biocompatible method compared to other synthesis methods (*i.e.*, chemical and physical).<sup>26,33</sup> Plant extracts contain phytochemicals (polyols, terpenoids, polyphenols, carboxylic acids, flavones, amides, *etc.*) that are capable of bioreducing metal ions to metal NPs.<sup>32,34,35</sup>

For the fabrication of NPs *via* green synthesis, most studies report the extraction of the substrate from plant matter, as shown in our previous study, where *Coffea arabica* seed (CAS) powder was used as a green precursor, where 50 mL of distilled water was mixed with 0.6 g of CAS power at 85 °C.<sup>28</sup> After this process, the extract was filtered and metallic salts were added. When the reducing agents from the CAS extract came in contact with the metal salts, a visual color change was observed (the color variation depends on the metal ions), revealing the formation of NPs.<sup>32,36</sup>

However, the reaction conditions such as the type of feedstock (microorganisms, plant material, *etc.*), temperature, pressure, pH, reaction time, reducing agent and metal ion concentration directly affect the chemical, physical, and optical characteristics (particle size, shape, and texture) of the nanoparticles.<sup>35,37–43</sup> For example, pH plays an essential role in the synthesis of NPs, affecting their size, shape, and reaction rate. Moreover, these nanoparticles are used for various applications, such as antimicrobial agents (*e.g.*, AgNPs),<sup>44,45</sup> cell imaging in cancer detection (*e.g.*, AuNPs),<sup>46</sup> alternative energy generation (*e.g.*, AuNPs),<sup>47,48</sup> remediation of oily sewage,<sup>49,50</sup> sensors (*e.g.*, AgNPs),<sup>51,52</sup> and moreover, as sustainable catalysts for environmental remediation (*e.g.*, AuNPs and AgNPs).<sup>28,53</sup> Environmental



Fig. 1 Schematic representing the history of publications from 2000–2022 (up to 8<sup>th</sup> March) on 4-nitrophenol/*p*-nitrophenol from Web of Science search results.



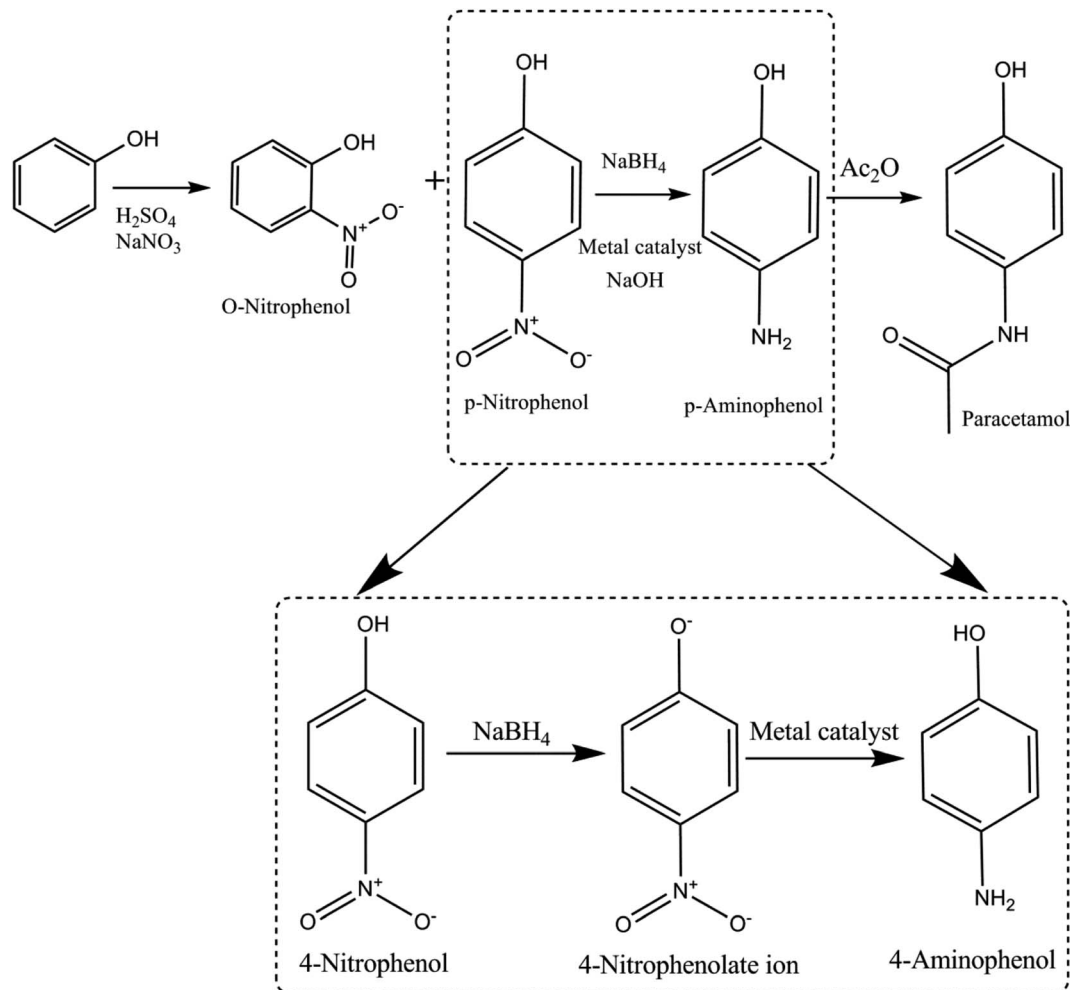


Fig. 2 Schematic representing the history of 4-nitrophenol acquired during the production of paracetamol from phenol as an intermediate product.

remediation has become important due to the negative impacts caused by pollution,<sup>54</sup> as mentioned above.<sup>55–67</sup> Water is one of the resources with the greatest impact due to the release of pollutants by industry and mining. Therefore, NPs obtained by green synthesis are an alternative for reducing toxic organic compounds (as mentioned in the Introduction). The possible mechanism for the formation of green-synthesized metal nanoparticles catalyst is still under debate. Various studies<sup>68–71</sup> have reported that the green precursors act as multifunctional agents with both reducing and capping capabilities, but limited efforts have been made to explore their chemistry. Some research groups proposed a possible understanding based on HPLC and FTIR results.

### 3.2 Catalyst characterization

The catalytic activity of metal nanoparticles depends on several properties, such as their synergistic effect, particle size, quantum effects, and surface properties. These properties can be investigated using several traditional characterization techniques. Primarily, the reduction of 4-NP is monitored using the absorption spectrum obtained by UV-visible absorbance

spectroscopy and to identify the electronic transition bands of metal nanoparticles.<sup>35</sup> The particle size of metal nanoparticles plays a significant role in the removal of 4-nitrophenol. These particle size measurements have been achieved using dynamic light scattering<sup>27</sup>-based particle size analyzers and high-resolution transmission electron microscopy.<sup>37</sup> As is known, the surface charge and functional groups present on the catalyst can improve the adsorption of the organic pollutant, followed by the fast catalyst reduction of 4-NP, which have been obtained from zeta potential and Fourier transform infrared spectroscopy (FT-IR) studies, respectively.<sup>39</sup>

## 4 Reduction of 4-nitrophenol using green-synthesized metal nanoparticles

### 4.1 Gold nanoparticles (AuNPs) as catalysts

Briefly, Xin Huang *et al.*<sup>72</sup> fabricated gold nanoparticles (AuNPs) for the first time using plant tannins. The resultant AuNPs were supported on the porous  $\gamma\text{-Al}_2\text{O}_3$ , and the formation of multiple hydrogen bonds with  $\gamma\text{-Al}_2\text{O}_3$  and self-cross-linking interactions among the stabilized AuNPs were observed. Further, the

fabricated Al<sub>2</sub>O<sub>3</sub>-AuNPs were used as a reusable catalyst to reduce 4-nitrophenol in aqueous medium. Initially, the Al<sub>2</sub>O<sub>3</sub>-AuNP catalyst was mixed with a 4-NP solution, which was bubbled with N<sub>2</sub> to remove the dissolved O<sub>2</sub> in the solution. Subsequently, NaBH<sub>4</sub> was added to the mixture, which initiated the catalytic reduction, and the reduction of 4-NP was monitored by measuring the characteristic absorption peak of 4-NP at 400 nm. In addition, the porous Al<sub>2</sub>O<sub>3</sub>-AuNPs exhibited better reusability than the conventional Au-Al<sub>2</sub>O<sub>3</sub> catalyst.

Daizy Philip's group<sup>86</sup> also proposed the fabrication of gold nanoparticles using an aqueous extract of fenugreek (*Trigonella foenum-graecum*) given that it is simple, efficient, economical, and nontoxic. The synthesized gold nanoparticles were characterized and tested for their size-dependent catalytic activity towards the reduction of 4-NP. The smaller nanoparticles showed faster activity.

Sanoe Chairam *et al.*<sup>88</sup> reported the preparation of mung bean starch (MBS)-mediated gold nanoparticles (AuNPs) through a green synthesis method, which were found to be efficient and recyclable catalysts for the reduction of 4-NP in the presence of NaBH<sub>4</sub>.

Recently, Mustaffa Shamsuddin's<sup>90</sup> group presented the use of thioctic acid-functionalized SiO<sub>2</sub>-coated Fe<sub>3</sub>O<sub>4</sub>-supported *P. macrocarpa* fruit extract-mediated AuNPs as a reusable catalyst for the reduction of 4-nitrophenol under various conditions. The optimization of the 4-nitrophenol reduction process was studied using the Box-Behnken design. Under the optimal conditions, the percentage reduction of 4-nitrophenol was 92% after 1 h, and the catalyst also maintained highly stable catalytic activity after five successive cycles.

Several other groups employed fungal *Aspergillus* sp. WL,<sup>73</sup> *Citrus maxima* (fruit),<sup>74</sup> fungus *Mariannaea* sp. HJ,<sup>75</sup> longan polysaccharides,<sup>76</sup> aspartame,<sup>77</sup> Jujube polysaccharides,<sup>78</sup> *Mimosa pudica* flower,<sup>79</sup> *Mimusops elengi* (bark),<sup>80</sup> *Cotoneaster horizontalis* leaves,<sup>81</sup> catechin-capped,<sup>82</sup> *Konjac glucomannan*,<sup>83</sup> caffeic acid,<sup>84</sup> *Coffea arabica* seed,<sup>20</sup> *Hedysarum* polysaccharides,<sup>87</sup> and *Sterculia acuminata* (fruit)<sup>68</sup> as precursors to obtain AuNPs (as an unsupported catalyst) for the reduction of 4-NP. The AuNPs obtained by green synthesis used to reduce 4-NP and their respective characteristics and reaction conditions are presented in Table 1.

**Table 1** AuNPs obtained by green synthesis used for the reduction of 4-NP with their respective characteristics and reaction conditions<sup>a</sup>

| Feedstock   | Size (nm) | Shape                                    | Reaction conditions          |                              |                 |            |  |
|---|-----------|--|------------------------------|------------------------------|-----------------|------------|--|
|   |           |  | Catalyst conc.               | NaBH <sub>4</sub> conc. (mM) | 4-NP conc. (mM) | Time (min) | Rate constant ( $K_{app}$ ) × 10 <sup>-3</sup> s <sup>-1</sup> |
| <b>Unsupported NPs</b>  |           |  |                              |                              |                 |            |  |
| Fungal <i>Aspergillus</i> sp. WL <sup>73</sup> (2017)   | 4–29      | Spherical                                | 114.72 mg L <sup>-1</sup>    | 30                           | 2               | 2–6        | 9.8–25 <sup>b</sup>  |
| <i>Citrus maxima</i> (fruit) <sup>74</sup> (2016)   | 25.7      | Rod and spherical                        | 1 mM                         | NR                           | 0.25            | 20         | 1.5 <sup>b</sup>   |
| Fungus <i>Mariannaea</i> sp. HJ <sup>75</sup> (2017)  | 11.7      | Spherical, hexagon, and irregular shapes | 0.195 g L <sup>-1</sup>      | 100                          | 2               | 3.3        | 24.7   |
| Longan polysaccharides <sup>76</sup> (2020)   | 7.8–15.6  | Spherical                                | 1.416 μM                     | 500                          | 0.6             | 42         | 4.65   |
| Aspartame <sup>77</sup> (2015)  | 1.2–50    | Spherical                                | 1.0 mM                       | 100                          | 4.0             | 9          | 6.84 <sup>b</sup>  |
| Mushroom <i>Pleurotus florida</i> <sup>78</sup> (2013)  | 5–16      | Spherical                                | 3.5 mg                       | 15                           | 2               | 30         | 1.9–33 <sup>b</sup>  |
| Jujube polysaccharides <sup>79</sup> (2019)   | 8–13      | Spherical and monodisperse               | 6.67 nM                      | NR                           | NR              | 18         | 1.17   |
| <i>Mimosa pudica</i> flower <sup>80</sup> (2017)  | ~24       | Spherical                                | 0.25 mM                      | 250                          | 5               | 15         | 5.0 <sup>b</sup>   |
| <i>Mimusops elengi</i> (bark) <sup>81</sup> (2016)  | 9–14      | Spherical                                | 0.42 mM                      | 13–14                        | 0.05            | 5–8        | 6.53–7.33  |
| <i>Cotoneaster horizontalis</i> leaves <sup>82</sup> (2017)   | 18        | Spherical                                | 1 mM                         | 30                           | 2               | 10         | NR   |
| Catechin-capped <sup>83</sup> (2014)  | 16.6      | Polydisperse                             | 0.5 mM                       | 5.5                          | 0.15            | 8.6        | 1.5 <sup>b</sup>   |
| Konjac glucomannan (KGM) <sup>84</sup> (2014)   | 12–31     | Uniform spherical                        | 10 mM                        | 10                           | 0.05            | 8.6        | 6.03   |
| Caffeic acid (CA) <sup>85</sup> (2017)  | 38.61     | Spherical                                | 0.2 mM                       | 200                          | 0.4             | 15         | 5.73   |
| <i>Coffea arabica</i> seed <sup>20</sup> (2018)   | 28        | Spherical                                | 10 mM                        | 100                          | 10              | 38         | 0.8 <sup>b</sup>   |
| <i>Trigonella foenum-graecum</i> <sup>86</sup> (2012)   | 15–25     | Spherical                                | 1.3 × 10 <sup>-4</sup> M     | 250                          | 0.25            | 7          | NR   |
| <i>Hedysarum</i> polysaccharides (HPS) <sup>87</sup> (2021)   | 5–8       | Spherical                                | 20 μL of 10% (stock Au salt) | 11.34 mg                     | 0.6             | 7          | NR   |
| <i>Sterculia acuminata</i> (fruit) <sup>68</sup> (2015)   | 26.5      | Spherical                                | 5 mM                         | 20                           | 1               | 36         | 1.8 <sup>b</sup>   |
| <b>Supported NPs</b>  |           |  |                              |                              |                 |            |  |
| Mung bean starch-AuNPs <sup>88</sup> (2017)   | 10        | Spherical                                | 20–100 mg                    | 0.1–0.9 g                    | 1               | 13         | 0.36 <sup>b</sup>  |
| Al <sub>2</sub> O <sub>3</sub> -Bayberry tannin-AuNPs <sup>89</sup> (2011)  | 4.63–5.08 | Spherical                                | 2.5 μM                       | 10                           | 0.2             | 5          | NR   |
| <i>Phaleria macrocarpa</i> (Scheff.) Boerl. ( <i>P. macrocarpa</i> ) AuNPs supported on -NH-SiO <sub>2</sub> -Fe <sub>3</sub> O <sub>4</sub> nanoparticles <sup>90</sup> (2020) | 2.4 ± 0.7 | Spherical                                | 2 mg                         | 100                          | 0.05            | 60         | NR   |

<sup>a</sup> NR = not reported. <sup>b</sup> Denoted values were recalculated for uniformity in the corresponding units with respect to other reports.



## 4.2 Silver nanoparticles (AgNPs) as catalysts

Abilash *et al.*<sup>91</sup> reported the use of *Breynia rhamnoides* stem extract-mediated spherical AgNPs to reduce 4-NP. The synthesized AgNPs exhibited relatively lower catalytic rates than Au NPs due to their relatively large size and the formation of a surface oxide layer. Further, Natarajan Sakthivel's group<sup>92</sup> reported the preparation of AgNPs using a fungus (*Cylindrocodium floridanum*), which were tested for the reduction of 4-NP as a homogeneous catalyst.

The reduction reaction rate was dependent on the reaction conditions such as concentration, size, and number of surface atoms of the catalyst. Later, Muniyappan *et al.*<sup>95</sup> fabricated silver nanoparticles using *Dalbergia spinosa* leaves and tested them to reduce 4-nitrophenol. In addition to absorbance studies, they used <sup>1</sup>H NMR spectroscopy to confirm the reduction of 4-nitrophenol and the formation of 4-aminophenol.

Recently, several other groups also devoted their efforts to the reduction of 4-nitrophenol using green-fabricated silver nanoparticles, such as *Psidium guajava* leaves,<sup>93</sup> Tulsi leaves,<sup>94</sup> polyphenol,<sup>97</sup> pestle curcumin,<sup>101</sup> seaweed *Fucus gardneri*,<sup>103</sup> and others.<sup>102–109</sup> The green-fabricated AgNPs used as catalysts to reduce 4-NP and their respective characteristics and reaction conditions are shown in Table 2.

## 4.3 Platinum and palladium nanoparticles as catalysts

In addition to Ag and Au nanoparticles, Pt and Pd NPs have been tested to reduce 4-NP to 4-AP with a similar mechanism understanding to that of Au and AgNPs. However, there are less reports on green-fabricated Pt and Pd NP-based 4-NP reduction probes than Ag and Au NPs. Generally, Pd and Pt NPs are among the most efficient catalysts for various organic reactions with fast reaction rates, high turnover frequency, and high yields.

Table 2 AgNPs obtained by green synthesis used for the reduction of 4-NP and their respective characteristics and reaction conditions<sup>a</sup>

| Feedstock  | Size (nm) | Shape                          | Reaction conditions                   |                              |                       |            |                       | Rate constant ( $K_{app}$ ) $\times 10^{-3} \text{ s}^{-1}$ | Ref. |
|--|-----------|--------------------------------|---------------------------------------|------------------------------|-----------------------|------------|-----------------------|---|------|
|  |           |                                | Catalyst conc.                        | NaBH <sub>4</sub> conc. (mM) | 4-NP conc. (mM)       | Time (min) |                       |   |      |
| <b>Unsupported NPs</b>   |           |                                |                                       |                              |                       |            |                       |   |      |
| <i>Psidium guajava</i> leaf (2019)   | 20–30     | Polydisperse                   | 10 $\mu\text{L}$                      | 100                          | 10                    | 8          | 2.6 <sup>b</sup>      | 93  |      |
| Fungus <i>Cylindrocodium floridanum</i> (2013)   | 25        | Quasi spherical                | 4.63–27.81 $\times 10^{-4} \text{ M}$ | 6.67                         | 0.1                   | 60         | 1.1 <sup>b</sup>      | 92  |      |
| Tulsi leaves (2018)  | 5–10      | Globular                       | 10 $\mu\text{L}$                      | 200                          | 5                     | 30         | 34.1 <sup>b</sup>     | 94  |      |
| <i>Dalbergia spinosa</i> leaves (2014)   | 18        | Quasi spherical                | 200 $\mu\text{L}$                     | 0.1                          | 0.1                   | NR         | NR                    | 95  |      |
| <i>Thymra spicata</i> leaves (2018)  | 7         | Spherical                      | 2 mg                                  | 250                          | 2                     | 60         | 64.5 <sup>b</sup>     | 96  |      |
| Polyphenol (2019)  | 2–10      | R                              | 0.2 mg L <sup>-1</sup>                | 10                           | 0.1                   | 16         | 2.8 <sup>b</sup>      | 97  |      |
| <i>Salmalia malabarica</i> gum (2016)  | 7         | Spherical                      | 10 $\mu\text{L}$                      | 15                           | 0.2                   | 60         | 0.9 <sup>b</sup>      | 98  |      |
| Kollicoat-capped Ag NPs (2016)   | ~20       | Spherical                      | 20 $\mu\text{L}$                      | 100                          | 0.1                   | 60         | NR                    | 99  |      |
| Leaf extract of <i>Peronema canescens</i> (2021)   | 19        | Spherical                      | 150 $\mu\text{L}$                     | 30                           | 2                     | 30         | NR                    | 100   |      |
| Pestle curcumin (2019)   | 15–40     | Spherical, rods, and hexagonal | 500 $\mu\text{L}$                     | 15                           | 0.15                  | 5          | NR                    | 101   |      |
| Extract of <i>Breynia rhamnoides</i> (2011)  | 27        | Spherical                      | 0.3 mL                                | 30                           | 2                     | ~7         | 9.19                  | 91  |      |
| <i>Sterculia acuminata</i> fruit (2016)  | 10–50     | Spherical                      | 10–100 $\mu\text{g mL}^{-1}$          | 0.1 N                        | 10 <sup>-4</sup> N    | 22         | 0.95 <sup>b</sup>     | 68  |      |
| <i>Stemona tuberosa</i> Lour (2018)  | 25        | Spherical                      | 20 $\mu\text{L}$                      | 1 mg                         | 1                     | 2880       | NR                    | 102   |      |
| Seaweed <i>Fucus gardneri</i> (2021)   | 19.39     | Quasi spherical                | 1 mg mL <sup>-1</sup>                 | 0.03                         | 2                     | 5          | 9.3 <sup>b</sup>      | 103   |      |
| <b>Supported NPs</b>   |           |                                |                                       |                              |                       |            |                       |   |      |
| Herbal tea from <i>Stachys lavandulifolia</i> (Fe <sub>3</sub> O <sub>4</sub> @S) (2018) | 20–40     | Quasi spherical                | 2 mg of catalyst (0.008 mol%)         | 0.3                          | 3                     | 0.5        | 63.4 <sup>b</sup>     | 104   |      |
| AgNPs decorated with hydroxyapatite (2018)   | 14.79     | Rod                            | 2 mg                                  | 200                          | 100                   | 9          | 2.0–7.3               | 105   |      |
| AgNPs decorated with SnO <sub>2</sub> microsphere (2017)                                 | 5         | Spherical                      | 1.5 mg                                | 1.5 mg                       | 20 mg L <sup>-1</sup> | 300–2160   | 4.7–51.7 <sup>b</sup> | 106   |      |
| AgNPs synthesized with polyphenols and supported on modified graphene (Ag-TPG) (2015)    | 5         | Spherical                      | 0.5 mg mL <sup>-1</sup>               | 10                           | 0.1                   | 13         | 3.35                  | 107   |      |
| AgNPs supported on cellulose nanocrystals (CNC@PDA-Ag) (2015)                            | ~10 nm    | R                              | 20 $\mu\text{g mL}^{-1}$              | 38                           | 0.12                  | 18         | 0.76 <sup>b</sup>     | 108   |      |
| AgNP-decorated halloysite nanotubes using dopamine (2018)                                | 10–20     | Rod                            | 1 g                                   | 200                          | 1                     | 7          | 4.45 <sup>b</sup>     | 109   |      |

<sup>a</sup> NR = not reported. <sup>b</sup> Denoted values were recalculated for uniformity in the corresponding units with respect to other reports.



However, the metal aggregation and precipitation result in catalyst decomposition and considerable loss in catalytic activity. Therefore, from the viewpoint of practical application, the use of green-fabricated Pd and Pt NP probes is desirable, similar to Au and Ag NPs.

When stable and uniform-sized Pd and Pt NPs are fabricated, they possess tremendous catalytic efficiency for the conversion of 4-nitrophenol to 4-aminophenol, better than other metal nanoparticles. In addition, our group found that self-assembled PtNPs demonstrated significant catalytic efficiency for the reduction of 4-NP. The rate constant of *Coffea arabica* seed-mediated self-assembled Pt nanoparticles ( $60 \times 10^{-3} \text{ s}^{-1}$ )<sup>70</sup> was almost two-times higher than that of mushroom *Pleurotus florida*-mediated AuNPs,<sup>78</sup> where due to the presence of sharp edges in their corners, the number of active surface sites in the anisotropic PtNPs is very high compared with bare NPs, and the small molecules from biomass could readily adsorb on the Pt surface.

For instance, even with only 5–50  $\mu\text{g}$  of *Sterculia acuminata*-mediated PdNPs,<sup>71</sup> the rate constant obtained was  $3.0 \times 10^{-3} \text{ s}^{-1}$ . The superior catalytic activity of Pd and Pt NPs than that of equivalent Au and Ag NPs may be attributed to several other properties, such as their particle size and electron structure on the surface of their atoms (encourages the temporary sticking of molecules). The overall electron cloud changes shape, allowing the stuck molecules to rearrange into new compounds; however, catalyst does not change. Subsequently, the rearranged molecules are eventually pushed out by new input ones (temperature-caused motion).

Several other green precursors such as guar gum,<sup>110</sup> sodium rhodizonate,<sup>111</sup> *Maytenus royleanus*,<sup>112</sup> *Sterculia Acuminata* fruit extract,<sup>69</sup> *Equisetum arvense* L/walnut shell,<sup>113</sup> and *Silybum marianum*<sup>114</sup> have been used to obtain Pt and PdNPs (as unsupported catalysts) for the reduction of 4-NP. Still, there is

room to develop supported catalysts using Pt/Pd NPs for the reduction of 4-NP. Table 3 shows the Pt and PdNPs obtained by green synthesis used to reduce 4-NP and their respective characteristics and reaction conditions.

#### 4.4 Bimetallic nanoparticles as catalysts

As is well known, the reduction of 4-nitrophenol using metal nanoparticles is mainly dependent on the size and shape of the NPs, and thus nanoengineering plays a crucial role in tailoring catalysts. Consequently, the presence of two or more metals in a single catalyst may increase the number of active sites in bimetal catalysts than single-metal catalysts. Also, there is the possibility of the synergistic effect in bimetal catalysts.<sup>115–127</sup>

In 2013, Bihua Xia *et al.*<sup>115</sup> presented green-fabricated spherical Au/Ag bimetallic nanoparticles using degraded *Pueraria mirifica* starch as both a reduction and stabilizing agent. Further, the authors tested the catalytic efficiency of the fabricated bimetallic Au/Ag nanoparticles towards the reduction of 4-nitrophenol. Interestingly, the Au/Ag bimetallic nanoparticles exhibited rapid 4-NP reduction reaction catalytic efficiency compared to the bare Ag and Au NPs. The reaction time for the Au/Ag bimetallic nanoparticles was almost 14-times higher than that for the mono metal NPs fabricated using the same degraded *Pueraria mirifica* starch. Similarly, the Daizy Philip group<sup>116</sup> reported the preparation of pomegranate fruit juice-mediated core-shell Au–Ag NPs and their use as catalysts for the reduction of 4-NP. They also obtained better catalytic efficiency with core-shell Au–Ag NPs than their monometallic NPs. The obtained apparent rate constant ( $13.3 \times 10^{-3} \text{ s}^{-1}$ ) of the core-shell Au–Ag nanoparticles was higher than that of the unsupported bimetal catalysts presented in the table.

The superior catalytic efficiency of bimetallic NPs may be due to the existence of two metals (Au and Ag) in their composition and their morphological changes, where due to their synergistic

Table 3 Platinum and palladium NPs obtained by green synthesis used for the reduction of 4-NP and their respective characteristics and reaction conditions<sup>a</sup>

| Feedstock  | Metal | Size (nm) | Shape               | Reaction conditions  |                              |                 |            |  | Ref. |  |
|--|-------|-----------|---------------------|----------------------|------------------------------|-----------------|------------|--|------|--|
|  |       |           |                     | Catalyst conc.       | NaBH <sub>4</sub> conc. (mM) | 4-NP conc. (mM) | Time (min) | Rate constant ( $K_{\text{app}} \times 10^{-3} \text{ s}^{-1}$ ) |      |  |
| <b>Platinum nanoparticles (PtNPs)</b>            |       |           |                     |                      |                              |                 |            |  |      |  |
| Guar gum (2014)                                  | Pt    | ~6        | Spherical           | 2.5 mM               | 100                          | 1               | 240        | 7  | 110  |  |
| Sodium rhodizonate (2018)                        | Pt    | 26        | Quasi spherical     | 50 $\mu\text{L}$     | 5 mg in 0.5 mL of water      | 0.2             | 10         | 18.1 <sup>b</sup>  | 111  |  |
| <i>Maytenus royleanus</i> (2017)                 | Pt    | 5–8       | Spherical           | 5 mg                 | 20                           | 1               | 20         | 2.1 <sup>b</sup>   | 112  |  |
| <i>Sterculia Acuminata</i> fruits extract (2018) | Pt    | ~3.4      | Irregular spherical | 10–100 $\mu\text{L}$ | 100                          | 2               | 8          | 0.1 <sup>b</sup>   | 69   |  |
| <i>Coffea Arabica</i> seed (2021)                | Pt    | 2         | Spherical           | 10 $\mu\text{L}$     | 0.76 mg                      | 1               | 3–5        | 60   | 70   |  |
| <b>Palladium nanoparticles (PdNPs)</b>           |       |           |                     |                      |                              |                 |            |  |      |  |
| <i>Equisetum arvense</i> L/walnut shell (2017)   | Pd    | 5–12      | Spherical           | 5 mg                 | 250                          | 2.5             | 1          | NR   | 113  |  |
| <i>Sterculia acuminata</i> (2018)                | Pd    | ~26.5     | Spherical           | 5–50 $\mu\text{g}$   | 100                          | 2               | 20         | 3.0  | 71   |  |
| <i>Silybum marianum</i> (2017)                   | Pd    | <20       | Spherical           | 0.5 mL               | 15                           | 20              | 27         | NR   | 114  |  |

<sup>a</sup> NR = Not Reported. <sup>b</sup> Denoted values were recalculated for uniformity in the corresponding units with respect to other reports.



effect, electrons can transfer from one metal to the other metal NPs (*i.e.*, the ionization potential of Au/Ag is 9.22/7.58 eV, respectively). This is important to enhance the electron cloud on the bimetallic NP surface in a kinetically favorable manner with more active sites. Table 4 demonstrates the bimetallic nanoparticles obtained by green synthesis to reduce 4-NP and their characteristics and reaction conditions.

Yinan Wang *et al.*<sup>117</sup> fabricated a template (*i.e.*, lipid as a tube-like template) based on palladium–platinum nanotubes using ascorbic acid. The fabricated Pd–Pt nanotubes (15  $\mu\text{g}$ ) showed an improved catalytic activity for the reduction of 4-NP. The calculated apparent rate constant ( $8.3 \times 10^{-3} \text{ s}^{-1}$ ) of Pd–Pt NTs was almost 2.5-times higher than that of the Pt NTs ( $3.3 \times 10^{-3} \text{ s}^{-1}$ ) presented in the same report. Furthermore, the fabricated Pd–Pt NTs were also tested for their recyclability over six cycles, and the authors did not observe any loss in their activity. Similar to the above-mentioned reports, the better catalytic efficiency of the PdPt NTs than Pt NTs is ascribed to the electron transfer effect.

Recently, Ye *et al.*<sup>126</sup> synthesized lichen-reduced graphene oxide (LrGO)–AgAu composites using *Cetraria islandica* (L.) Ach. Extract. The fabricated LrGO–AgAu nanocomposites were examined for the reduction of 4-NP. Similar to previous reports on bimetallic NPs, higher catalytic activity was observed for the

reduction of 4-NP than that with the monometallic nanocomposites related to the preparation of small-sized homogeneous particles, which give a significant amount of active sites on the nanocomposite surface.

The superior catalytic activity of bimetallic nanoparticles than that of monometallic nanoparticles may be attributed to several other properties, such as the synergic effect, particle size, quantum effects, and surface properties of the metal nanoparticles. Alternatively, rapid and easy procedures are essential to improve the reusability of catalytic probes.

#### 4.5 Suggested studies during the 4-nitrophenol reduction process

**4.5.1 Effect of  $\text{NaBH}_4$  concentration on 4-nitrophenol reduction.** According to Fig. 2,  $\text{NaBH}_4$  plays a vital role in the reduction of 4-NP. However, besides the rigorous reaction, at higher concentration, it leads to toxicity due to the presence of boron. Even though numerous studies employed higher concentrations of  $\text{NaBH}_4$  than 4-NP to achieve a higher reaction rate and get a perfect fit in the pseudo-first-order reaction plot during the process, it is time to think about the Environmental Protection Agency (EPA)/World Health Organization (WHO) toxicity limit of boron, which is supposed to be under 2.4  $\mu\text{g}$

Table 4 Bimetallic nanoparticles obtained by green synthesis used for the reduction of 4-NP and their respective characteristics and reaction conditions<sup>115–127a</sup>

| Feedstock   | Metal             | Size (nm) | Shape           | Reaction conditions       |                            |                      |            |  |      |
|---|-------------------|-----------|-----------------|---------------------------|----------------------------|----------------------|------------|--|------|
|   |                   |           |                 | Catalyst conc.            | $\text{NaBH}_4$ conc. (mM) | 4-NP conc. (mM)      | Time (min) | Rate constant ( $K_{\text{app}} \times 10^{-3} \text{ s}^{-1}$ ) | Ref. |
| <b>Unsupported NPs</b>  |                   |           |                 |                           |                            |                      |            |  |      |
| Ascorbic acid (2019)  | Pd–Pt             | ~57       | Nanotubes       | 15 $\mu\text{g}$          | 100                        | 0.009                | 10         | 3.4 <sup>b</sup>   | 117  |
| <i>Morganella psychrotolerans</i> and <i>Desulfovibrio alaskensis</i> (2019)                    | Pd–Pt             | NR        | NR              | 0.1 mM                    | 10                         | 0.1                  | 10         | NR   | 118  |
| Waste tea leaves extract (2021)   | Ag–Au             | 20        | Spherical       | 20 $\mu\text{L}$          | 20 $\mu\text{L}$           | 0.1                  | 6–7        | NR   | 119  |
| <i>Pulicaria undulata</i> (2020)  | Au–Ag             | 5–12      | Spherical       | 0.3 mL                    | 30                         | 2                    | ~5         | NR   | 120  |
| <i>Salvia officinalis</i> (2021)  | Ag–Fe             | 30        | Quasi spherical | 5 mg                      | 20                         | 0.2                  | 45         | 1.1 <sup>b</sup>   | 121  |
| Polysaccharide extracted from <i>Ramaria botrytis</i> mushroom (2020)                           | Ag–Au             | 150       | Spherical       | 30.27 mg $\text{mL}^{-1}$ | 30                         | 0.057                | 14         | 3.6 <sup>b</sup>   | 122  |
| <i>Punica granatum</i> extract (2015)   | Au–Ag             | 12        | Core–shell      | NR                        | 100                        | 5                    | 6          | 13.3 <sup>b</sup>  | 123  |
| <i>Silybum marianum</i> seed extract (2015)   | Au–Ag             | 20–200    | Spherical       | 0.5 mL                    | 15                         | 2                    | 24         | NR   | 124  |
| <i>Ginger rhizome</i> powder (2018)   | Cu–Ag Cu–Ni       | NR        | Spherical       | 10 mg                     | 500                        | 1                    | 10         | 4.05–6.08  | 125  |
| NPs supported on degraded <i>Pueraria mirifica</i> starch (DPS) (2013)                          | Au–Ag             | 1.6–26    | Spherical       | 0.3 mL                    | 15                         | 0.2                  | 35         | NR   | 116  |
| <b>Supported NPs</b>  |                   |           |                 |                           |                            |                      |            |  |      |
| NPs synthesized with <i>Cetraria islandica</i> (L.) ash and supported on graphene oxides (2020) | Ag–Au (LrGO–AgAu) | 6–30      | Spherical       | 2.7 mL                    | 100                        | $9.6 \times 10^{-5}$ | 2–3        | 7.5–11.4   | 126  |
| NPs supported on polydopamine-functionalized graphene (2016)                                    | Pt–Au             | 2.7–6     | Spherical       | 3 mg $\text{mL}^{-1}$     | 100                        | 0.1                  | 16         | 9.5  | 127  |
| NPs decorated on graphene nanosheets (2014)   | Au–Pd             | 2.67–3.15 | Spherical       | 1.25 $\mu\text{g}$        | 10                         | 0.1                  | 25         | 14.5   | 115  |

<sup>a</sup> NR = not reported. <sup>b</sup> Denoted values were recalculated for uniformity in the corresponding units with respect to other reports.



$\text{mL}^{-1}$ .<sup>1,128</sup> Obviously, the catalytic reduction reaction may take more time if the concentration of  $\text{NaBH}_4$  is lower, but it is essential to evade boron purification.

**4.5.2 Effect of reaction temperature on 4-nitrophenol reduction.** To determine the ability of green-fabricated metal catalysts for 4-NP reduction, it is necessary to consider environmental conditions and it is essential to perform temperature-dependent studies. Based on the temperature-dependent 4-NP reduction reaction kinetics, we can also estimate thermodynamic parameters such as entropy, enthalpy, and Gibbs free energy. Sanoo Chairam *et al.*<sup>88</sup> tested mung bean starch-mediated AuNPs for the reduction of 4-NP at different temperatures and calculated the activation energy ( $E_a$ ), enthalpy and entropy of  $47.42 \text{ kJ mol}^{-1}$ ,  $44.78 \text{ kJ mol}^{-1}$ , and  $261.49 \text{ kJ mol}^{-1}$ , respectively.

**4.5.3 Experiments mimicking environmental conditions.** To test the efficiency of the fabricated catalysts, the reaction needs to be performed in real (river, marine, agriculture, industry, *etc.*) water samples. As mentioned in the introduction, 4-NP is also used as a pH indicator, and thus the real water samples contain different pH and several contaminants such as metal ions and pesticides. Thus, the changes in the absorption spectrum can confirm the pH of the real water solution. As is well known, the faster catalytic reduction of 4-NP happens in basic pH medium. On the one hand, there is a possibility of undergoing a faster reaction rate in real water samples (most samples above neutral pH). On the other hand, slower reaction kinetics can be observed due to the presence of unwanted systems such as heavy metals and other pollutants.

Moreover, interference studies need to be performed before using NPs in real-world applications. To the best of our knowledge, there are no studies on real water sample testing using green-fabricated metal nanoparticles.

#### 4.6 Catalytic performance estimation parameters

The kinetics of the reaction can be estimated using the pseudo-first-order reaction, as follows:

$$\ln(C_t/C_0) = -kt$$

The regression factor ( $R^2$ ) and rate of the reaction can be obtained from the slope ( $k$ , units:  $\text{s}^{-1}$  or  $\text{min}^{-1}$ ).

$$\ln(C_t/C_0) \text{ vs. } t$$

where,  $C_0$  and  $C_t$  indicate the initial and concentration of 4-NP at time  $t$ , respectively, and  $k$  is the apparent rate constant.

Thermodynamic parameters

$$\text{Gibbs free energy } (\Delta G) = \Delta H - T\Delta S \quad (1)$$

From the Arrhenius equation

$$\ln(k) = \left(-\frac{E_a}{R}\right) \frac{1}{T} + \ln(A) \quad (2)$$

$$\ln(k) \text{ vs. } \frac{1}{T}$$

and

$$-\frac{E_a}{R} = \text{slope}$$

Eyring equation

$$\ln\left(\frac{k}{T}\right) = \left(-\frac{\Delta H}{R}\right) \frac{1}{T} + \ln\left(\frac{K_B}{h}\right) + \frac{\Delta S}{R} \quad (3)$$

$$\ln\left(\frac{k}{T}\right) \text{ vs. } \frac{1}{T}; \left(-\frac{\Delta H}{R}\right) = \text{slope}$$

and

$$\ln\left(\frac{K_B}{h}\right) + \frac{\Delta S}{R} = \text{constant } (c)$$

where  $A$  = Arrhenius constant, change in enthalpy ( $\Delta H$ ) and entropy,  $R = 8.314 \text{ J k}^{-1} \text{ mol}^{-1}$ ,  $K_B = 1.381 \times 10^{-23} \text{ J k}^{-1}$ ,  $h = 6.626 \times 10^{-34} \text{ J k}^{-1} \text{ mol}^{-1}$ ,  $T$  = absolute temperature in Kelvin, and  $k = k_{\text{app}}$  = pseudo-first-order rate constant.

Activity parameter

$$k' = k/m \text{ units: } \text{s}^{-1} \text{ mg}^{-1}$$

where  $m$  is the catalyst mass and  $k$  rate of the reaction.

Reduction/degradation capacity

$$Q_t = (C_0 - C_t) \times M/m$$

where  $C_0$  is the initial and  $C_t$  is the concentration of 4-NP at time  $t$ ,  $m$  is the mass of the catalyst and  $M$  is the mass of the organic pollutant.

Turnover number (TON): the TON is calculated using the number of moles of substrate that 1 mol of catalyst can convert into product.

Turnover frequency (TOF): the TOF is calculated simply by TON/reaction time.

Conversion efficiency

$$\text{Conversion efficiency } (\%) = \frac{C_0 - C_t}{C_0} \times 100$$

where  $C_0$  and  $C_t$  are the initial absorbance of the 4-nitrophenol solution and with time ( $t$ ), respectively.

## 5 Possible mechanistic understanding for the conversion of 4-nitrophenol to 4-aminophenol

The catalytic reduction of 4-NP by  $\text{NaBH}_4$  and metal catalysts was investigated with the possible reaction mechanism presented in Fig. 3 initially following the LH model. The ionization of sodium borohydride in the liquid phase results in the production of borohydride ions ( $\text{BH}_4^-$ ) and their adsorption on the surface of the metal catalyst to form a metal hydride







Fig. 3 Possible understanding of the conversion of 4-nitrophenol to 4-aminophenol using NaBH<sub>4</sub> and metal nanoparticles as an H<sub>2</sub> source and catalyst, respectively.

complex.<sup>20,27,70,75,78</sup> Simultaneously, 4-nitrophenol adsorbs on the metal hydride complex surface. Given that the progress is reversible, adsorption is followed by the desorption process. Thermodynamic equilibrium on the hydride complex surface allows H<sub>2</sub> transfer from the hydride complex surface to 4-NP, followed by the formation of the 4-nitrophenolate ion (4-NP<sup>-</sup>).

Even though the specific mechanism still needs to be understood, according to the available hypothetical concepts, two (direct and condensation) paths can be proposed for the conversion of 4-nitrophenol to 4-aminophenol in the presence of NaBH<sub>4</sub> and catalyst. In the direct path, there is a possibility to obtain two consecutive fast reactions, *i.e.*, nitro group to nitroso group formation, and then amine group. Similarly, the condensation path involves the formation of azoxy compounds through the condensation of hydroxylamine with the nitroso compound. This is followed by its reduction, azoxy to hydrazo and hydrazo to 4-AP.

## 6 Challenges and future perspectives

In conclusion, green-fabricated metal nanoparticles and their up-to-date advancements in the reduction of 4-nitrophenol exhibited escalated progress in the past two decades. However, some challenges still need to be addressed for their possible scalability and application as economically viable water purifiers. Besides the production approach for developing highly stable and efficient metal nanoparticles, absorption in the entire visible spectrum and narrow bandwidth of metal nanoparticles with monodispersity and uniformity are required for specific applications and enhanced catalytic activity. Incredibly, researchers are still struggling to find possible economically viable techniques/methods for purifying metal nanoparticles and confirming the reduction of 4-nitrophenol.

The use of green materials from recycled waste needs to be assessed to produce metal nanoparticles. In addition, it is necessary to understand the effect of the presence of biomass

on the development of metal nanoparticles. Alternatively, rapid and simple procedures are essential to develop recyclable catalytic probes to boost catalytic efficiency. We suppose that the forthcoming investigation of catalytic probes using sustainable precursor-based metal nanoparticles will expand the general audience and scientific community awareness of their pollution removal application because of their simplicity, accessibility, and compatibility.

## Conflicts of interest

There are no conflicts to declare.

## References

- 1 United States Environmental Protection Agency, *Ambient Water, Quality Criteria for Nitrophenols*, 1980.
- 2 P. Deka, D. Bhattacharjee, P. Sarmah, R. C. Deka and P. Bharali, Catalytic Reduction of Water Contaminant '4-Nitrophenol' over Manganese Oxide Supported Ni Nanoparticles, in *Trends Asian Water Environ. Sci. Technol.*, Springer International Publishing, Cham, 2017, pp. 35–48, DOI: [10.1007/978-3-319-39259-2\\_3](https://doi.org/10.1007/978-3-319-39259-2_3).
- 3 T. Achamo and O. P. Yadav, Removal of 4-Nitrophenol from Water Using Ag-N-PTrioped TiO<sub>2</sub> by Photocatalytic Oxidation Technique, *Anal. Chem. Insights*, 2016, **2016**, 29–34, DOI: [10.4137/Aci.s31508](https://doi.org/10.4137/Aci.s31508).
- 4 R. D. Neal, Y. Inoue, R. A. Hughes and S. Neretina, Catalytic Reduction of 4-Nitrophenol by Gold Catalysts: The Influence of Borohydride Concentration on the Induction Time, *J. Phys. Chem. C*, 2019, **123**, 12894–12901, DOI: [10.1021/acs.jpcc.9b02396](https://doi.org/10.1021/acs.jpcc.9b02396).
- 5 J. Zhang, G. Chen, D. Guay, M. Chaker and D. Ma, Highly active PtAu alloy nanoparticle catalysts for the reduction of 4-nitrophenol, *Nanoscale*, 2014, **6**, 2125–2130, DOI: [10.1039/c3nr04715f](https://doi.org/10.1039/c3nr04715f).



- 6 Y.-T. Woo and D. Y. Lai, Aromatic Amino and Nitro-Amino Compounds and Their Halogenated Derivatives, in *Patty's Toxicol.*, John Wiley & Sons, Inc., Hoboken, NJ, USA, 2012, pp. 1–96, DOI: [10.1002/0471435139.tox058.pub2](https://doi.org/10.1002/0471435139.tox058.pub2).
- 7 N. F. Abd Razak and M. Shamsuddin, Catalytic reduction of 4-nitrophenol over biostabilized gold nanoparticles supported onto thioctic acid functionalized silica-coated magnetite nanoparticles and optimization using response surface methodology, *Inorg. Nano-Met. Chem.*, 2020, **50**, 489–500, DOI: [10.1080/24701556.2020.1720724](https://doi.org/10.1080/24701556.2020.1720724).
- 8 N. K. R. Bogireddy, P. Sahare, U. Pal, S. F. O. Méndez, L. M. Gomez and V. Agarwal, Platinum nanoparticle-assembled porous biogenic silica 3D hybrid structures with outstanding 4-nitrophenol degradation performance, *Chem. Eng. J.*, 2020, **388**, 124237, DOI: [10.1016/j.cej.2020.124237](https://doi.org/10.1016/j.cej.2020.124237).
- 9 W. Shen, Y. Qu, X. Pei, S. Li, S. You, J. Wang, Z. Zhang and J. Zhou, Catalytic reduction of 4-nitrophenol using gold nanoparticles biosynthesized by cell-free extracts of *Aspergillus* sp. WL-Au, *J. Hazard. Mater.*, 2017, **321**, 299–306, DOI: [10.1016/j.jhazmat.2016.07.051](https://doi.org/10.1016/j.jhazmat.2016.07.051).
- 10 Z. Xiong, H. Zhang, W. Zhang, B. Lai and G. Yao, Removal of nitrophenols and their derivatives by chemical redox: a review, *Chem. Eng. J.*, 2019, **359**, 13–31, DOI: [10.1016/j.cej.2018.11.111](https://doi.org/10.1016/j.cej.2018.11.111).
- 11 P. Zhao, X. Feng, D. Huang, G. Yang and D. Astruc, Basic concepts and recent advances in nitrophenol reduction by gold- and other transition metal nanoparticles, *Coord. Chem. Rev.*, 2015, **287**, 114–136, DOI: [10.1016/j.ccr.2015.01.002](https://doi.org/10.1016/j.ccr.2015.01.002).
- 12 E. Menumero, R. A. Hughes and S. Neretina, Catalytic Reduction of 4-Nitrophenol: A Quantitative Assessment of the Role of Dissolved Oxygen in Determining the Induction Time, *Nano Lett.*, 2016, **16**, 7791–7797, DOI: [10.1021/acs.nanolett.6b03991](https://doi.org/10.1021/acs.nanolett.6b03991).
- 13 S. J. Lee, Y. Yu, H. J. Jung, S. S. Naik, S. Yeon and M. Y. Choi, Efficient recovery of palladium nanoparticles from industrial wastewater and their catalytic activity toward reduction of 4-nitrophenol, *Chemosphere*, 2021, **262**, 128358, DOI: [10.1016/j.chemosphere.2020.128358](https://doi.org/10.1016/j.chemosphere.2020.128358).
- 14 M. T. Islam, R. Saenz-Arana, H. Wang, R. Bernal and J. C. Noveron, Green synthesis of gold, silver, platinum, and palladium nanoparticles reduced and stabilized by sodium rhodizonate and their catalytic reduction of 4-nitrophenol and methyl orange, *New J. Chem.*, 2018, **42**, 6472–6478, DOI: [10.1039/c8nj01223g](https://doi.org/10.1039/c8nj01223g).
- 15 M. Khan, K. Al-Hamoud, Z. Liaqat, M. R. Shaik, S. F. Adil, M. Kuniyil, H. Z. Alkhatlan, A. Al-Warthan, M. R. H. Siddiqui, M. Mondeshki, W. Tremel, M. Khan and M. N. Tahir, Synthesis of au, ag, and au–ag bimetallic nanoparticles using pulicaria undulata extract and their catalytic activity for the reduction of 4-nitrophenol, *Nanomaterials*, 2020, **10**, 1–14, DOI: [10.3390/nano10091885](https://doi.org/10.3390/nano10091885).
- 16 N. Arora, A. Mehta, A. Mishra and S. Basu, 4-Nitrophenol reduction catalysed by Au–Ag bimetallic nanoparticles supported on LDH: homogeneous vs. heterogeneous catalysis, *Appl. Clay Sci.*, 2018, **151**, 1–9, DOI: [10.1016/j.clay.2017.10.015](https://doi.org/10.1016/j.clay.2017.10.015).
- 17 S. Pandey and S. B. Mishra, Catalytic reduction of *p*-nitrophenol by using platinum nanoparticles stabilised by guar gum, *Carbohydr. Polym.*, 2014, **113**, 525–531, DOI: [10.1016/j.carbpol.2014.07.047](https://doi.org/10.1016/j.carbpol.2014.07.047).
- 18 J. Jiang, G. H. Gunasekar, S. Park, S. H. Kim, S. Yoon and L. Piao, Hierarchical Cu nanoparticle-aggregated cages with high catalytic activity for reduction of 4-nitrophenol and carbon dioxide, *Mater. Res. Bull.*, 2018, **100**, 184–190, DOI: [10.1016/j.materresbull.2017.12.018](https://doi.org/10.1016/j.materresbull.2017.12.018).
- 19 N. K. R. Bogireddy, U. Pal, L. M. Gomez and V. Agarwal, Size controlled green synthesis of gold nanoparticles using *Coffea arabica* seed extract and their catalytic performance in 4-nitrophenol reduction, *RSC Adv.*, 2018, **8**, 24819–24826, DOI: [10.1039/c8ra04332a](https://doi.org/10.1039/c8ra04332a).
- 20 M. I. Din, R. Khalid, Z. Hussain, T. Hussain, A. Mujahid, J. Najeeb and F. Izhar, Nanocatalytic Assemblies for Catalytic Reduction of Nitrophenols: A Critical Review, *Crit. Rev. Anal. Chem.*, 2020, **50**, 322–338, DOI: [10.1080/10408347.2019.1637241](https://doi.org/10.1080/10408347.2019.1637241).
- 21 P. Zhao, X. Feng, D. Huang, G. Yang and D. Astruc, Basic concepts and recent advances in nitrophenol reduction by gold- and other transition metal nanoparticles, *Coord. Chem. Rev.*, 2015, **287**, 114–136.
- 22 M. Teimouri, F. Khosravi-Nejad, F. Attar, A. A. Saboury, I. Kostova, G. Benelli and M. Falahati, Gold nanoparticles fabrication by plant extracts: synthesis, characterization, degradation of 4-nitrophenol from industrial wastewater, and insecticidal activity—a review, *J. Cleaner Prod.*, 2018, **184**, 740–753.
- 23 N. Pradhan, A. Pal and T. Pal, Silver nanoparticle catalyzed reduction of aromatic nitro compounds, *Colloids Surf., A*, 2002, **196**, 247–257.
- 24 Y. Li, Y. Cao, J. Xie, D. Jia, H. Qin and Z. Liang, Facile solid-state synthesis of Ag/graphene oxide nanocomposites as highly active and stable catalyst for the reduction of 4-nitrophenol, *Catal. Commun.*, 2015, **58**, 21–25, DOI: [10.1016/j.catcom.2014.08.022](https://doi.org/10.1016/j.catcom.2014.08.022).
- 25 S. Fountoulaki, V. Daikopoulou, P. L. Gkizis, I. Tamiolakis, G. S. Armatas and I. N. Lykakis, Mechanistic studies of the reduction of nitroarenes by NaBH<sub>4</sub> or hydrosilanes catalyzed by supported gold nanoparticles, *ACS Catal.*, 2014, **4**, 3504–3511, DOI: [10.1021/cs500379u](https://doi.org/10.1021/cs500379u).
- 26 J. Singh, T. Dutta, K. H. Kim, M. Rawat, P. Samddar and P. Kumar, “Green” synthesis of metals and their oxide nanoparticles: applications for environmental remediation, *J. Nanobiotechnol.*, 2018, **16**, 1–24, DOI: [10.1186/s12951-018-0408-4](https://doi.org/10.1186/s12951-018-0408-4).
- 27 N. K. R. Bogireddy and V. Agarwal, *Persea americana* seed extract mediated gold nanoparticles for mercury(ii)/iron(iii) sensing, 4-nitrophenol reduction, and organic dye degradation, *RSC Adv.*, 2019, **9**, 39834–39842, DOI: [10.1039/c9ra08233f](https://doi.org/10.1039/c9ra08233f).
- 28 N. K. R. Bogireddy, U. Pal, M. K. Kumar, J. M. Domínguez, L. M. Gomez and V. Agarwal, Green fabrication of 2D platinum superstructures and their high catalytic activity



- for mitigation of organic pollutants, *Catal. Today*, 2021, **360**, 185–193, DOI: [10.1016/j.cattod.2019.06.044](https://doi.org/10.1016/j.cattod.2019.06.044).
- 29 E. Burlacu, C. Tanase, N. A. Coman and L. Berta, A review of bark-extract-mediated green synthesis of metallic nanoparticles and their applications, *Molecules*, 2019, **24**, 1–18, DOI: [10.3390/molecules24234354](https://doi.org/10.3390/molecules24234354).
- 30 S. Ahmed, M. Ahmad, B. L. Swami and S. Ikram, A review on plants extract mediated synthesis of silver nanoparticles for antimicrobial applications: a green expertise, *J. Adv. Res.*, 2016, **7**, 17–28, DOI: [10.1016/j.jare.2015.02.007](https://doi.org/10.1016/j.jare.2015.02.007).
- 31 S. Ahmad, S. Munir, N. Zeb, A. Ullah, B. Khan, J. Ali, M. Bilal, M. Omer, M. Alamzeb, S. M. Salman and S. Ali, Green nanotechnology: a review on green synthesis of silver nanoparticles—an ecofriendly approach, *Int. J. Nanomed.*, 2019, **14**, 5087–5107, DOI: [10.2147/IJN.S200254](https://doi.org/10.2147/IJN.S200254).
- 32 S. Jadoun, R. Arif, N. K. Jangid and R. K. Meena, Green synthesis of nanoparticles using plant extracts: a review, *Environ. Chem. Lett.*, 2021, **19**, 355–374, DOI: [10.1007/s10311-020-01074-x](https://doi.org/10.1007/s10311-020-01074-x).
- 33 C. F. Carolin, P. S. Kumar, A. Saravanan, G. J. Joshiba and M. Naushad, Efficient techniques for the removal of toxic heavy metals from aquatic environment: a review, *J. Environ. Chem. Eng.*, 2017, **5**, 2782–2799, DOI: [10.1016/j.jece.2017.05.029](https://doi.org/10.1016/j.jece.2017.05.029).
- 34 N. K. R. Bogireddy, Y. R. Mejia, T. M. Aminabhavi, V. Barba, R. H. Becerra, A. D. A. Flores and V. Agarwal, *J. Environ. Manage.*, 2022, **316**, 115292, DOI: [10.1016/j.jenvman.2022.115292](https://doi.org/10.1016/j.jenvman.2022.115292).
- 35 S. Irvani, Green synthesis of metal nanoparticles using plants, *Green Chem.*, 2011, **13**, 2638–2650, DOI: [10.1039/c1gc15386b](https://doi.org/10.1039/c1gc15386b).
- 36 K. F. Princy and A. Gopinath, Green synthesis of silver nanoparticles using polar seaweed *Fucus gardeneri* and its catalytic efficacy in the reduction of nitrophenol, *Polar Sci.*, 2021, 100692, DOI: [10.1016/j.polar.2021.100692](https://doi.org/10.1016/j.polar.2021.100692).
- 37 G. S. Dhillon, S. K. Brar, S. Kaur and M. Verma, Green approach for nanoparticle biosynthesis by fungi: current trends and applications, *Crit. Rev. Biotechnol.*, 2012, **32**, 49–73, DOI: [10.3109/07388551.2010.550568](https://doi.org/10.3109/07388551.2010.550568).
- 38 A. Rana, K. Yadav and S. Jagadevan, A comprehensive review on green synthesis of nature-inspired metal nanoparticles: mechanism, application and toxicity, *J. Cleaner Prod.*, 2020, **272**, 122880, DOI: [10.1016/j.jclepro.2020.122880](https://doi.org/10.1016/j.jclepro.2020.122880).
- 39 H. Duan, D. Wang and Y. Li, Green chemistry for nanoparticle synthesis, *Chem. Soc. Rev.*, 2015, **44**, 5778–5792, DOI: [10.1039/c4cs00363b](https://doi.org/10.1039/c4cs00363b).
- 40 M. Gericke and A. Pinches, Biological synthesis of metal nanoparticles, *Hydrometallurgy*, 2006, **83**, 132–140, DOI: [10.1016/j.hydromet.2006.03.019](https://doi.org/10.1016/j.hydromet.2006.03.019).
- 41 D. S. Shen, J. Mathew and D. Philip, Photosynthesis of Au, Ag and Au-Ag bimetallic nanoparticles using aqueous extract and dried leaf of *Anacardium occidentale*, *Spectrochim. Acta, Part A*, 2011, **79**, 254–262, DOI: [10.1016/j.saa.2011.02.051](https://doi.org/10.1016/j.saa.2011.02.051).
- 42 M. Rezaayat, R. K. Blundell, J. E. Camp, D. A. Walsh and W. Thielemans, Green one-step synthesis of catalytically active palladium nanoparticles supported on cellulose nanocrystals, *ACS Sustainable Chem. Eng.*, 2014, **2**, 1241–1250, DOI: [10.1021/sc500079q](https://doi.org/10.1021/sc500079q).
- 43 G. A. Kahrilas, L. M. Wally, S. J. Fredrick, M. Hiskey, A. L. Prieto and J. E. Owens, Microwave-assisted green synthesis of silver nanoparticles using orange peel extract, *ACS Sustainable Chem. Eng.*, 2014, **2**, 367–376, DOI: [10.1021/sc4003664](https://doi.org/10.1021/sc4003664).
- 44 R. Banasiuk, M. Krychowiak, D. Swigon, W. Tomaszewicz, A. Michalak, A. Chylewska, M. Ziabka, M. Lapinski, B. Koscielska, M. Narajczyk and A. Krolicka, Carnivorous plants used for green synthesis of silver nanoparticles with broad-spectrum antimicrobial activity, *Arabian J. Chem.*, 2017, **13**, 1415–1428, DOI: [10.1016/j.arabjc.2017.11.013](https://doi.org/10.1016/j.arabjc.2017.11.013).
- 45 S. Jebiril, R. Khanfir Ben Jenana and C. Dridi, Green synthesis of silver nanoparticles using *Melia azedarach* leaf extract and their antifungal activities: In vitro and in vivo, *Mater. Chem. Phys.*, 2020, **248**, 122898, DOI: [10.1016/j.matchemphys.2020.122898](https://doi.org/10.1016/j.matchemphys.2020.122898).
- 46 J. G. Wang, S. S. Jang, D. S. H. Wong, S. S. Shieh and C. W. Wu, Soft-sensor development with adaptive variable selection using nonnegative garrote, *Control Eng. Pract.*, 2013, **21**, 1157–1164, DOI: [10.1016/j.conengprac.2013.05.006](https://doi.org/10.1016/j.conengprac.2013.05.006).
- 47 A. A. Basheer and I. Ali, Water photo splitting for green hydrogen energy by green nanoparticles, *Int. J. Hydrogen Energy*, 2019, **44**, 11564–11573, DOI: [10.1016/j.ijhydene.2019.03.040](https://doi.org/10.1016/j.ijhydene.2019.03.040).
- 48 I. Khan, K. Saeed and I. Khan, Nanoparticles: Properties, applications and toxicities, *Arab. J. Chem.*, 2019, **12**, 908–931, DOI: [10.1016/j.arabjc.2017.05.011](https://doi.org/10.1016/j.arabjc.2017.05.011).
- 49 E. Murgueitio, L. Cumbal, M. Abril, A. Izquierdo, A. Debut and O. Tinoco, Síntesis verde de nanopartículas de hierro: aplicación en la eliminación de aceite de petróleo de agua y suelos contaminados, *J. Nanotechnol.*, 2018, **2018**, 1–288.
- 50 Y. Peng, Y. Liu, J. Dai, L. Cao and X. Liu, A sustainable strategy for remediation of oily sewage: Clean and safe, *Sep. Purif. Technol.*, 2020, **240**, 116592, DOI: [10.1016/j.seppur.2020.116592](https://doi.org/10.1016/j.seppur.2020.116592).
- 51 A. Yakoh, P. Rattanarat, W. Siangproh and O. Chailapakul, Simple and selective paper-based colorimetric sensor for determination of chloride ion in environmental samples using label-free silver nanoprisms, *Talanta*, 2018, **178**, 134–140, DOI: [10.1016/j.talanta.2017.09.013](https://doi.org/10.1016/j.talanta.2017.09.013).
- 52 V. Kumar, D. K. Singh, S. Mohan, D. Bano, R. K. Gundampati and S. H. Hasan, *Green synthesis of silver nanoparticle for the selective and sensitive colorimetric detection of mercury (II) ion*, Elsevier B.V., 2017, DOI: [10.1016/j.jphotobiol.2017.01.022](https://doi.org/10.1016/j.jphotobiol.2017.01.022).
- 53 L. Castro, M. L. Blázquez, F. González, J. A. Muñoz and A. Ballester, Heavy metal adsorption using biogenic iron compounds, *Hydrometallurgy*, 2018, **179**, 44–51, DOI: [10.1016/j.hydromet.2018.05.029](https://doi.org/10.1016/j.hydromet.2018.05.029).
- 54 Y. Wang, D. O'Connor, Z. Shen, I. M. C. Lo, D. C. W. Tsang, S. Pehkonen, S. Pu and D. Hou, Green synthesis of nanoparticles for the remediation of contaminated waters



- and soils: constituents, synthesizing methods, and influencing factors, *J. Cleaner Prod.*, 2019, **226**, 540–549, DOI: [10.1016/j.jclepro.2019.04.128](https://doi.org/10.1016/j.jclepro.2019.04.128).
- 55 E. K. F. Elbeshehy, A. M. Elazzazy and G. Aggelis, Silver nanoparticles synthesis mediated by new isolates of *Bacillus* spp., nanoparticle characterization and their activity against Bean Yellow Mosaic Virus and human pathogens, *Front. Microbiol.*, 2015, **6**, 1–13, DOI: [10.3389/fmicb.2015.00453](https://doi.org/10.3389/fmicb.2015.00453).
- 56 P. Singh, Y. J. Kim, C. Wang, R. Mathiyalagan and D. C. Yang, Microbial synthesis of Flower-shaped gold nanoparticles, *Artif. Cells, Nanomed., Biotechnol.*, 2016, **44**, 1469–1474, DOI: [10.3109/21691401.2015.1041640](https://doi.org/10.3109/21691401.2015.1041640).
- 57 P. Singh, Y. J. Kim, C. Wang, R. Mathiyalagan and D. C. Yang, *Weissella oryzae* DC6-facilitated green synthesis of silver nanoparticles and their antimicrobial potential, *Artif. Cells, Nanomed., Biotechnol.*, 2016, **44**, 1569–1575, DOI: [10.3109/21691401.2015.1064937](https://doi.org/10.3109/21691401.2015.1064937).
- 58 K. Kalaivani, Biosynthesis of Silver Nanoparticles Using *Lactobacillus Acidophilus* and White Rot Fungus-A Comparative Study, *Int. J. Adv. Res. Ideas Innov. Technol.*, 2017, **3**, 299–306.
- 59 M. Gericke and A. Pinches, Biological synthesis of metal nanoparticles, *Hydrometallurgy*, 2006, **83**, 132–140, DOI: [10.1016/j.hydromet.2006.03.019](https://doi.org/10.1016/j.hydromet.2006.03.019).
- 60 B. Sharma, D. D. Purkayastha, S. Hazra, M. Thajamanbi, C. R. Bhattacharjee, N. N. Ghosh and J. Rout, Biosynthesis of fluorescent gold nanoparticles using an edible freshwater red alga, *Lemanea fluviatilis* (L.) C.Ag. and antioxidant activity of biomatrix loaded nanoparticles, *Bioprocess Biosyst. Eng.*, 2014, **37**, 2559–2565, DOI: [10.1007/s00449-014-1233-2](https://doi.org/10.1007/s00449-014-1233-2).
- 61 Y. Abboud, T. Saffaj, A. Chagraoui, A. El Bouari, K. Brouzi, O. Tanane and B. Ihssane, Biosynthesis, characterization and antimicrobial activity of copper oxide nanoparticles (CONPs) produced using brown alga extract (*Bifurcaria bifurcata*), *Appl. Nanosci.*, 2014, **4**, 571–576, DOI: [10.1007/s13204-013-0233-x](https://doi.org/10.1007/s13204-013-0233-x).
- 62 J. Annamalai and T. Nallamuthu, Characterization of biosynthesized gold nanoparticles from aqueous extract of *Chlorella vulgaris* and their anti-pathogenic properties, *Appl. Nanosci.*, 2015, **5**, 603–607, DOI: [10.1007/s13204-014-0353-y](https://doi.org/10.1007/s13204-014-0353-y).
- 63 T. Kathiraven, A. Sundaramanickam, N. Shanmugam and T. Balasubramanian, Green synthesis of silver nanoparticles using marine algae *Caulerpa racemosa* and their antibacterial activity against some human pathogens, *Appl. Nanosci.*, 2015, **5**, 499–504, DOI: [10.1007/s13204-014-0341-2](https://doi.org/10.1007/s13204-014-0341-2).
- 64 D. S. Shen, J. Mathew and D. Philip, Photosynthesis of Au, Ag and Au-Ag bimetallic nanoparticles using aqueous extract and dried leaf of *Anacardium occidentale*, *Spectrochim. Acta, Part A*, 2011, **79**, 254–262, DOI: [10.1016/j.saa.2011.02.051](https://doi.org/10.1016/j.saa.2011.02.051).
- 65 M. Rezaayat, R. K. Blundell, J. E. Camp, D. A. Walsh and W. Thielemans, Green one-step synthesis of catalytically active palladium nanoparticles supported on cellulose nanocrystals, *ACS Sustainable Chem. Eng.*, 2014, **2**, 1241–1250, DOI: [10.1021/sc500079q](https://doi.org/10.1021/sc500079q).
- 66 G. A. Kahrilas, L. M. Wally, S. J. Fredrick, M. Hiskey, A. L. Prieto and J. E. Owens, Microwave-assisted green synthesis of silver nanoparticles using orange peel extract, *ACS Sustainable Chem. Eng.*, 2014, **2**, 367–376, DOI: [10.1021/sc4003664](https://doi.org/10.1021/sc4003664).
- 67 N. S. Al-Radadi and S. I. Y. Adam, Green biosynthesis of Pt-nanoparticles from Anbara fruits: toxic and protective effects on CCl<sub>4</sub> induced hepatotoxicity in Wister rats, *Arabian J. Chem.*, 2020, **13**, 4386–4403, DOI: [10.1016/j.arabjc.2019.08.008](https://doi.org/10.1016/j.arabjc.2019.08.008).
- 68 N. K. R. Bogireddy, K. K. Hoskote Anand and B. K. Mandal, Gold Nanoparticles – Synthesis by *Sterculia Acuminata* Extract and Its Catalytic Efficiency in Alleviating Different Organic Dyes, *J. Mol. Liq.*, 2015, **211**, 868–875, DOI: [10.1016/j.molliq.2015.07.027](https://doi.org/10.1016/j.molliq.2015.07.027).
- 69 N. K. R. Bogireddy, H. A. Kiran Kumar and B. K. Mandal, Biofabricated silver nanoparticles as green catalyst in the degradation of different textile dyes, *J. Environ. Chem. Eng.*, 2016, **4**, 56–64, DOI: [10.1016/j.jece.2015.11.004](https://doi.org/10.1016/j.jece.2015.11.004).
- 70 N. K. R. Bogireddy, U. Pal, M. K. Kumar, J. M. Domínguez, L. M. Gomez and V. Agarwal, Green Fabrication of 2D Platinum Superstructures and Their High Catalytic Activity for Mitigation of Organic Pollutants, *Catal. Today*, 2021, **360**, 185–193, DOI: [10.1016/j.cattod.2019.06.044](https://doi.org/10.1016/j.cattod.2019.06.044).
- 71 N. K. R. Bogireddy, K. K. Hoskote Anand and B. K. Mandal, Catalytic Efficiency of Green Synthesized Palladium Nanoparticles by *Sterculia Acuminata* Extract towards Abatement of Organic Pollutants, *Biointerface Res. Appl. Chem.*, 2018, **8**(3), 3319–3323.
- 72 X. Huang, X. Liao and B. Shi, Synthesis of Highly Active and Reusable Supported Gold Nanoparticles and Their Catalytic Applications to 4-Nitrophenol Reduction, *Green Chem.*, 2011, **13**(10), 2801–2805, DOI: [10.1039/c1gc15873b](https://doi.org/10.1039/c1gc15873b).
- 73 W. Shen, Y. Qu, X. Pei, S. Li, S. You, J. Wang, Z. Zhang and J. Zhou, Catalytic Reduction of 4-Nitrophenol Using Gold Nanoparticles Biosynthesized by Cell-Free Extracts of *Aspergillus* Sp. WL-Au, *J. Hazard. Mater.*, 2017, **321**, 299–306, DOI: [10.1016/j.jhazmat.2016.07.051](https://doi.org/10.1016/j.jhazmat.2016.07.051).
- 74 J. Yu, D. Xu, H. N. Guan, C. Wang, L. K. Huang and D. F. Chi, Facile One-Step Green Synthesis of Gold Nanoparticles Using Citrus Maxima Aqueous Extracts and Its Catalytic Activity, *Mater. Lett.*, 2016, **166**(26), 110–112, DOI: [10.1016/j.matlet.2015.12.031](https://doi.org/10.1016/j.matlet.2015.12.031).
- 75 X. Pei, Y. Qu, W. Shen, H. Li, X. Zhang, S. Li, Z. Zhang and X. Li, Green Synthesis of Gold Nanoparticles Using Fungus *Mariannaea* Sp. HJ and Their Catalysis in Reduction of 4-Nitrophenol, *Environ. Sci. Pollut. Res.*, 2017, **24**(27), 21649–21659, DOI: [10.1007/s11356-017-9684-z](https://doi.org/10.1007/s11356-017-9684-z).
- 76 X. Zhang, L. Fan, Y. Cui, T. Cui, S. Chen, G. Ma, W. Hou and L. Wang, Green Synthesis of Gold Nanoparticles Using Longan Polysaccharide and Their Reduction of 4-Nitrophenol and Biological Applications, *Nano*, 2020, **15**, 1–8, DOI: [10.1142/S1793292020500022](https://doi.org/10.1142/S1793292020500022).
- 77 S. Wu, S. Yan, W. Qi, R. Huang, J. Cui, R. Su and Z. He, Green Synthesis of Gold Nanoparticles Using Aspartame



- and Their Catalytic Activity for P-Nitrophenol Reduction, *Nanoscale Res. Lett.*, 2015, **10**(1), 6, DOI: [10.1186/s11671-015-0910-7](https://doi.org/10.1186/s11671-015-0910-7).
- 78 I. K. Sen, K. Maity and S. S. Islam, Green Synthesis of Gold Nanoparticles Using a Glucan of an Edible Mushroom and Study of Catalytic Activity, *Carbohydr. Polym.*, 2013, **91**(2), 518–528, DOI: [10.1016/j.carbpol.2012.08.058](https://doi.org/10.1016/j.carbpol.2012.08.058).
- 79 Y. Cui, X. Guo, X. Lai, H. Sun, B. Liang, W. Hou, X. Liu and L. Wang, Green Synthesis of Jujube-Polysaccharide-Stabilized Gold Nanoparticles for Reduction of 4-Nitrophenol, *ChemistrySelect*, 2019, **4**(39), 11483–11487, DOI: [10.1002/slct.201902531](https://doi.org/10.1002/slct.201902531).
- 80 K. Mapala and M. Pattabi, Mimosa Pudica Flower Extract Mediated Green Synthesis of Gold Nanoparticles, *NanoWorld J.*, 2017, **3**(2), 44–50, DOI: [10.17756/nwj.2017-045](https://doi.org/10.17756/nwj.2017-045).
- 81 R. Majumdar, B. G. Bag and P. Ghosh, Mimosaops Elengi Bark Extract Mediated Green Synthesis of Gold Nanoparticles and Study of Its Catalytic Activity, *Appl. Nanosci.*, 2016, **6**(4), 521–528, DOI: [10.1007/s13204-015-0454-2](https://doi.org/10.1007/s13204-015-0454-2).
- 82 S. Khan, W. Runguo, K. Tahir, Z. Jichuan and L. Zhang, Catalytic Reduction of 4-Nitrophenol and Photo Inhibition of Pseudomonas Aeruginosa Using Gold Nanoparticles as Photocatalyst, *J. Photochem. Photobiol., B*, 2017, **170**, 181–187, DOI: [10.1016/j.jphotobiol.2017.04.006](https://doi.org/10.1016/j.jphotobiol.2017.04.006).
- 83 Y. Choi, M. J. Choi, S. H. Cha, Y. S. Kim, S. Cho and Y. Park, Catechin-Capped Gold Nanoparticles: Green Synthesis, Characterization, and Catalytic Activity toward 4-Nitrophenol Reduction, *Nanoscale Res. Lett.*, 2014, **9**(1), 1–8, DOI: [10.1186/1556-276X-9-103](https://doi.org/10.1186/1556-276X-9-103).
- 84 Z. Gao, R. Su, R. Huang, W. Qi and Z. He, Glucomannan-Mediated Facile Synthesis of Gold Nanoparticles for Catalytic Reduction of 4-Nitrophenol, *Nanoscale Res. Lett.*, 2014, **9**(1), 1–8, DOI: [10.1186/1556-276X-9-404](https://doi.org/10.1186/1556-276X-9-404).
- 85 Y. S. Seo, E. Y. Ahn, J. Park, T. Y. Kim, J. E. Hong, K. Kim, Y. Park and Y. Park, Catalytic Reduction of 4-Nitrophenol with Gold Nanoparticles Synthesized by Caffeic Acid, *Nanoscale Res. Lett.*, 2017, **12**(1), 1–11, DOI: [10.1186/s11671-016-1776-z](https://doi.org/10.1186/s11671-016-1776-z).
- 86 S. Aswathy Aromal and D. Philip, Green Synthesis of Gold Nanoparticles Using Trigonella Foenum-Graecism and Its Size-Dependent Catalytic Activity, *Spectrochim. Acta, Part A*, 2012, **97**, 1–5, DOI: [10.1016/j.saa.2012.05.083](https://doi.org/10.1016/j.saa.2012.05.083).
- 87 X. Chen, Z. Xue, J. Ji, D. Wang, G. Shi, L. Zhao and S. Feng, Hedysarum Polysaccharides Mediated Green Synthesis of Gold Nanoparticles and Study of Its Characteristic, Analytical Merit, Catalytic Activity, *Mater. Res. Bull.*, 2021, **133**(2020), 111070, DOI: [10.1016/j.materresbull.2020.111070](https://doi.org/10.1016/j.materresbull.2020.111070).
- 88 S. Chairam, W. Konkamdee and R. Parakhun, Starch-Supported Gold Nanoparticles and Their Use in 4-Nitrophenol Reduction Starch-Supported Gold Nanoparticles in 4-Nitrophenol Reduction, *J. Saudi Chem. Soc.*, 2017, **21**(6), 656–663, DOI: [10.1016/j.jscs.2015.11.001](https://doi.org/10.1016/j.jscs.2015.11.001).
- 89 X. Huang, X. Liao and B. Shi, Synthesis of Highly Active and Reusable Supported Gold Nanoparticles and Their Catalytic Applications to 4-Nitrophenol Reduction, *Green Chem.*, 2011, **13**(10), 2801–2805, DOI: [10.1039/c1gc15873b](https://doi.org/10.1039/c1gc15873b).
- 90 N. F. Abd Razak and M. Shamsuddin, Catalytic reduction of 4-nitrophenol over biostabilized gold nanoparticles supported onto thioctic acid functionalized silicacoated magnetite nanoparticles and optimization using response surface methodology, *Inorg. Nano-Met. Chem.*, 2020, **50**, 1–14, DOI: [10.1080/24701556.2020.1720724](https://doi.org/10.1080/24701556.2020.1720724).
- 91 A. Gangula, R. Podila, R. M. L. Karanam, C. Janardhana and A. M. Rao, Catalytic reduction of 4-nitrophenol using biogenic gold and silver nanoparticles derived from breynia rhamnoides, *Langmuir*, 2011, **27**, 15268–15274, DOI: [10.1021/la2034559](https://doi.org/10.1021/la2034559).
- 92 K. B. Narayanan, H. H. Park and N. Sakthivel, Extracellular synthesis of mycogenic silver nanoparticles by *Cylindrocladium floridanum* and its homogeneous catalytic degradation of 4-nitrophenol, *Spectrochim. Acta, Part A*, 2013, **116**, 485–490, DOI: [10.1016/j.saa.2013.07.066](https://doi.org/10.1016/j.saa.2013.07.066).
- 93 J. Kaur, J. Singh and M. Rawat, An efficient and blistering reduction of 4-nitrophenol by green synthesized silver nanoparticles, *SN Appl. Sci.*, 2019, **1**, 1–6, DOI: [10.1007/s42452-019-1088-x](https://doi.org/10.1007/s42452-019-1088-x).
- 94 J. Singh, A. Mehta, M. Rawat and S. Basu, Green synthesis of silver nanoparticles using sun dried tulsi leaves and its catalytic application for 4-Nitrophenol reduction, *J. Environ. Chem. Eng.*, 2018, **6**, 1468–1474, DOI: [10.1016/j.jece.2018.01.054](https://doi.org/10.1016/j.jece.2018.01.054).
- 95 N. Muniyappan and N. S. Nagarajan, Green synthesis of silver nanoparticles with *Dalbergia spinosa* leaves and their applications in biological and catalytic activities, *Process Biochem.*, 2014, **49**, 1054–1061, DOI: [10.1016/j.procbio.2014.03.015](https://doi.org/10.1016/j.procbio.2014.03.015).
- 96 H. Veisi, S. Azizi and P. Mohammadi, Green synthesis of the silver nanoparticles mediated by *Thymbra spicata* extract and its application as a heterogeneous and recyclable nanocatalyst for catalytic reduction of a variety of dyes in water, *J. Cleaner Prod.*, 2018, **170**, 1536–1543, DOI: [10.1016/j.jclepro.2017.09.265](https://doi.org/10.1016/j.jclepro.2017.09.265).
- 97 Z. Wang, Y. Huang, D. Lv, G. Jiang, F. Zhang and A. Song, Tea polyphenol-assisted green synthesis of Ag-nanodiamond hybrid and its catalytic activity towards 4-nitrophenol reduction, *Green Chem. Lett. Rev.*, 2019, **12**, 197–207, DOI: [10.1080/17518253.2019.1624836](https://doi.org/10.1080/17518253.2019.1624836).
- 98 I. Murali Krishna, G. Bhagavanth Reddy, G. Veerabhadram and A. Madhusudhan, Eco-friendly green synthesis of silver nanoparticles using *salmalia malabarica*: synthesis, characterization, antimicrobial, and catalytic activity studies, *Appl. Nanosci.*, 2016, **6**, 681–689, DOI: [10.1007/s13204-015-0479-6](https://doi.org/10.1007/s13204-015-0479-6).
- 99 M. Sharma, A. Mishra, V. Kumar and S. Basu, Green Synthesis of Silver Nanoparticles with Exceptional Colloidal Stability and its Catalytic Activity Toward Nitrophenol Reduction, *Nano*, 2016, **11**, 1–10, DOI: [10.1142/S1793292016500466](https://doi.org/10.1142/S1793292016500466).
- 100 S. Salprima Yudha, A. Falahudin, R. H. Wibowo, J. Hendri and D. O. Wicaksono, Reduction of 4-nitrophenol mediated by silver nanoparticles synthesized using



- aqueous leaf extract of *Peronema canescens*, *Bull. Chem. React. Eng. Catal.*, 2021, **16**, 253–259, DOI: [10.9767/bcrec.16.2.10426.253-259](https://doi.org/10.9767/bcrec.16.2.10426.253-259).
- 101 D. S. Al-Namil, E. El Khoury and D. Patra, Solid-State Green Synthesis of Ag NPs: Higher Temperature Harvests Larger Ag NPs but Smaller Size Has Better Catalytic Reduction Reaction, *Sci. Rep.*, 2019, **9**, 1–9, DOI: [10.1038/s41598-019-51693-w](https://doi.org/10.1038/s41598-019-51693-w).
- 102 B. Bonigala, B. Kasukurthi, V. V. Konduri, U. K. Mangamuri, R. Gorrepati and S. Poda, Green synthesis of silver and gold nanoparticles using *Stemona tuberosa* Lour and screening for their catalytic activity in the degradation of toxic chemicals, *Environ. Sci. Pollut. Res.*, 2018, **25**, 32540–32548, DOI: [10.1007/s11356-018-3105-9](https://doi.org/10.1007/s11356-018-3105-9).
- 103 K. F. Princy and A. Gopinath, Green synthesis of silver nanoparticles using polar seaweed *Fucus gardeneri* and its catalytic efficacy in the reduction of nitrophenol, *Polar Sci.*, 2021, 100692, DOI: [10.1016/j.polar.2021.100692](https://doi.org/10.1016/j.polar.2021.100692).
- 104 M. Shahriary, H. Veisi, M. Hekmati and S. Hemmati, In situ green synthesis of Ag nanoparticles on herbal tea extract (*Stachys lavandulifolia*)-modified magnetic iron oxide nanoparticles as antibacterial agent and their 4-nitrophenol catalytic reduction activity, *Mater. Sci. Eng., C*, 2018, **90**, 57–66, DOI: [10.1016/j.msec.2018.04.044](https://doi.org/10.1016/j.msec.2018.04.044).
- 105 T. K. Das, S. Ganguly, P. Bhawal, S. Mondal and N. C. Das, A facile green synthesis of silver nanoparticle-decorated hydroxyapatite for efficient catalytic activity towards 4-nitrophenol reduction, *Res. Chem. Intermed.*, 2018, **44**, 1189–1208, DOI: [10.1007/s11164-017-3161-7](https://doi.org/10.1007/s11164-017-3161-7).
- 106 M. Hu, Z. Zhang, C. Luo and X. Qiao, One-Pot Green Synthesis of Ag-Decorated SnO<sub>2</sub> Microsphere: an Efficient and Reusable Catalyst for Reduction of 4-Nitrophenol, *Nanoscale Res. Lett.*, 2017, **12**, 1–10, DOI: [10.1186/s11671-017-2204-8](https://doi.org/10.1186/s11671-017-2204-8).
- 107 Z. Wang, C. Xu, X. Li and Z. Liu, In situ green synthesis of Ag nanoparticles on tea polyphenols-modified graphene and their catalytic reduction activity of 4-nitrophenol, *Colloids Surf., A*, 2015, **485**, 102–110, DOI: [10.1016/j.colsurfa.2015.09.015](https://doi.org/10.1016/j.colsurfa.2015.09.015).
- 108 J. Tang, Z. Shi, R. M. Berry and K. C. Tam, Mussel-inspired green metallization of silver nanoparticles on cellulose nanocrystals and their enhanced catalytic reduction of 4-nitrophenol in the presence of  $\beta$ -cyclodextrin, *Ind. Eng. Chem. Res.*, 2015, **54**, 3299–3308, DOI: [10.1021/acs.iecr.5b00177](https://doi.org/10.1021/acs.iecr.5b00177).
- 109 T. K. Das, S. Ganguly, P. Bhawal, S. Remanan, S. Mondal and N. C. Das, Mussel inspired green synthesis of silver nanoparticles-decorated halloysite nanotube using dopamine: Characterization and evaluation of its catalytic activity, *Appl. Nanosci.*, 2018, **8**, 173–186, DOI: [10.1007/s13204-018-0658-3](https://doi.org/10.1007/s13204-018-0658-3).
- 110 S. Pandey and S. B. Mishra, Catalytic Reduction of P-Nitrophenol by Using Platinum Nanoparticles Stabilised by Guar Gum, *Carbohydr. Polym.*, 2014, **113**, 525–531, DOI: [10.1016/j.carbpol.2014.07.047](https://doi.org/10.1016/j.carbpol.2014.07.047).
- 111 M. T. Islam, R. Saenz-Arana, H. Wang, R. Bernal and J. C. Noveron, Green Synthesis of Gold, Silver, Platinum, and Palladium Nanoparticles Reduced and Stabilized by Sodium Rhizonate and Their Catalytic Reduction of 4-Nitrophenol and Methyl Orange, *New J. Chem.*, 2018, **42**(8), 6472–6478, DOI: [10.1039/c8nj01223g](https://doi.org/10.1039/c8nj01223g).
- 112 S. Ullah, A. Ahmad, A. Wang, M. Raza, A. U. Jan, K. Tahir, A. U. Rahman and Y. Qipeng, Bio-Fabrication of Catalytic Platinum Nanoparticles and Their in Vitro Efficacy against Lungs Cancer Cells Line (A549), *J. Photochem. Photobiol., B*, 2017, **173**, 368–375, DOI: [10.1016/j.jphotobiol.2017.06.018](https://doi.org/10.1016/j.jphotobiol.2017.06.018).
- 113 M. Bordbar and N. Mortazavimanes, Green Synthesis of Pd/Walnut Shell Nanocomposite Using Equisetum Arvense L. Leaf Extract and Its Application for the Reduction of 4-Nitrophenol and Organic Dyes in a Very Short Time, *Environ. Sci. Pollut. Res.*, 2017, **24**(4), 4093–4104, DOI: [10.1007/s11356-016-8183-y](https://doi.org/10.1007/s11356-016-8183-y).
- 114 R. Gopalakrishnan, B. Loganathan, S. Dinesh and K. Raghu, Strategic Green Synthesis, Characterization and Catalytic Application to 4-Nitrophenol Reduction of Palladium Nanoparticles, *J. Cluster Sci.*, 2017, **28**(4), 2123–2131, DOI: [10.1007/s10876-017-1207-z](https://doi.org/10.1007/s10876-017-1207-z).
- 115 B. Xia, F. He and L. Li, Preparation of Bimetallic Nanoparticles Using a Facile Green Synthesis Method and Their Application, *Langmuir*, 2013, **29**(15), 4901–4907, DOI: [10.1021/la400355u](https://doi.org/10.1021/la400355u).
- 116 M. Meena Kumari, J. Jacob and D. Philip, Green Synthesis and Applications of Au-Ag Bimetallic Nanoparticles, *Spectrochim. Acta, Part A*, 2015, **137**, 185–192, DOI: [10.1016/j.saa.2014.08.079](https://doi.org/10.1016/j.saa.2014.08.079).
- 117 Y. Wang, Q. Li, P. Zhang, D. O'Connor, R. S. Varma, M. Yu and D. Hou, One-Pot Green Synthesis of Bimetallic Hollow Palladium-Platinum Nanotubes for Enhanced Catalytic Reduction of p-Nitrophenol, *J. Colloid Interface Sci.*, 2019, **539**, 161–167, DOI: [10.1016/j.jcis.2018.12.053](https://doi.org/10.1016/j.jcis.2018.12.053).
- 118 M. J. Capeness, V. Echavarrri-Bravo and L. E. Horsfall, Production of Biogenic Nanoparticles for the Reduction of 4-Nitrophenol and Oxidative Laccase-like Reactions, *Front. Microbiol.*, 2019, **10**, 1–9, DOI: [10.3389/fmicb.2019.00997](https://doi.org/10.3389/fmicb.2019.00997).
- 119 C. W. Kang and H. Kolya, Green Synthesis of Ag-Au Bimetallic Nanocomposites Using Waste Tea Leaves Extract for Degradation Congo Red and 4-Nitrophenol, *Sustain*, 2021, **13**(6), 1–9, DOI: [10.3390/su13063318](https://doi.org/10.3390/su13063318).
- 120 M. Khan, K. Al-Hamoud, Z. Liaqat, M. R. Shaik, S. F. Adil, M. Kuniyil, H. Z. Alkhatlan, A. Al-Warthan, M. R. H. Siddiqui, M. Mondeshki, W. Tremel, M. Khan and M. N. Tahir, Synthesis of Au, Ag, and Au-Ag Bimetallic Nanoparticles Using *Pulicaria Undulata* Extract and Their Catalytic Activity for the Reduction of 4-Nitrophenol, *Nanomaterials*, 2020, **10**(9), 1–14, DOI: [10.3390/nano10091885](https://doi.org/10.3390/nano10091885).
- 121 M. A. Malik, A. A. Alshehri and R. Patel, Facile One-Pot Green Synthesis of Ag-Fe Bimetallic Nanoparticles and Their Catalytic Capability for 4-Nitrophenol Reduction, *J.*



- Mater. Res. Technol.*, 2021, **12**, 455–470, DOI: [10.1016/j.jmrt.2021.02.063](https://doi.org/10.1016/j.jmrt.2021.02.063).
- 122 S. K. Bhanja, S. K. Samanta, B. Mondal, S. Jana, J. Ray, A. Pandey and T. Tripathy, Green Synthesis of Ag@Au Bimetallic Composite Nanoparticles Using a Polysaccharide Extracted from Ramaria Botrytis Mushroom and Performance in Catalytic Reduction of 4-Nitrophenol and Antioxidant, Antibacterial Activity, *Environ. Nanotechnol., Monit. Manage.*, 2020, **14**, 100341, DOI: [10.1016/j.enmm.2020.100341](https://doi.org/10.1016/j.enmm.2020.100341).
- 123 R. Gopalakrishnan, B. Loganathan and K. Raghu, Green Synthesis of Au-Ag Bimetallic Nanocomposites Using Silybum Marianum Seed Extract and Their Application as a Catalyst, *RSC Adv.*, 2015, **5**(40), 31691–31699, DOI: [10.1039/c5ra03571f](https://doi.org/10.1039/c5ra03571f).
- 124 M. Ismail, M. I. Khan, S. B. Khan, M. A. Khan, K. Akhtar and A. M. Asiri, Green Synthesis of Plant Supported Cu–Ag and Cu–Ni Bimetallic Nanoparticles in the Reduction of Nitrophenols and Organic Dyes for Water Treatment, *J. Mol. Liq.*, 2018, **260**, 78–91, DOI: [10.1016/j.molliq.2018.03.058](https://doi.org/10.1016/j.molliq.2018.03.058).
- 125 Z. Çıplak, B. Getiren, C. Gökalp, A. Yıldız and N. Yıldız, Green Synthesis of Reduced Graphene Oxide-AgAu Bimetallic Nanocomposite: Catalytic Performance, *Chem. Eng. Commun.*, 2020, **207**(4), 559–573, DOI: [10.1080/00986445.2019.1613227](https://doi.org/10.1080/00986445.2019.1613227).
- 126 W. Ye, J. Yu, Y. Zhou, D. Gao, D. Wang, C. Wang and D. Xue, Green Synthesis of Pt-Au Dendrimer-like Nanoparticles Supported on Polydopamine-Functionalized Graphene and Their High Performance toward 4-Nitrophenol Reduction, *Appl. Catal., B*, 2016, **181**, 371–378, DOI: [10.1016/j.apcatb.2015.08.013](https://doi.org/10.1016/j.apcatb.2015.08.013).
- 127 X. Chen, X. Chen, Z. Cai and M. Oyama, AuPd Bimetallic Nanoparticles Decorated on Graphene Nanosheets: Their Green Synthesis, Growth Mechanism and High Catalytic Ability in 4-Nitrophenol Reduction, *J. Mater. Chem. A*, 2014, **2**(16), 5668–5674, DOI: [10.1039/c3ta15141g](https://doi.org/10.1039/c3ta15141g).
- 128 N. K. R. Bogireddy, R. C. Silva, M. A. Valenzuela and V. Agarwal, 4-nitrophenol optical sensing with N doped oxidized carbon dots, *J. Hazard. Mater.*, 2020, **386**, 121643, DOI: [10.1016/j.jhazmat.2019.121643](https://doi.org/10.1016/j.jhazmat.2019.121643).

